

Design and synthesis of fluorescence-labeled *closo*-dodecaborate lipid: its liposome formation and *in vivo* imaging targeting of tumors for boron neutron capture therapy†

Hiroyuki Nakamura,* Noriko Ueda, Hyun Seung Ban, Manabu Ueno and Shoji Tachikawa

Received 1st September 2011, Accepted 1st November 2011

DOI: 10.1039/c1ob06500a

The fluorescence-labeled *closo*-dodecaborane lipid (FL-SBL) was synthesized from (S)-(+)-1,2-isopropylidene-glycerol as a chiral starting material. FL-SBL was readily accumulated into the PEGylated DSPC liposomes prepared from DSPC, CH, and DSPE-PEG-OMe by the post insertion protocol. The boron concentrations and the fluorescent intensities of the FL-SBL-labeled DSPC liposomes increased with the increase of the additive FL-SBL, and the maximum emission wavelength of the liposomes appeared at 531 nm. A preliminary *in vivo* imaging study of tumor-bearing mice revealed that the FL-SBL-labeled DSPC liposomes were delivered to the tumor tissue but not distributed to hypoxic regions.

Introduction

Since the discovery of the enhanced permeability and retention (EPR) effect by Maeda and Matsumura in 1986,^{1,2} much attention has been focused on drug delivery systems (DDS) using drug-embedded nano carriers including liposomes, micelles, proteinaceous or polymer-conjugated macromolecules, and lipid particles.^{3,4} The EPR effect is based on the abnormal architectures and impaired functional regulation of newly formed tumoral blood vessels, and this phenomena will lead to abnormal molecular and fluid transport dynamics especially for macromolecular species.^{5,6}

This nano carrier-based DDS is also an attractive approach for efficient boron delivery systems (BDS) to tumors for boron neutron capture therapy (BNCT). BNCT is a bimodal therapy reliant on the selective uptake and/or retention of sensitizing boron molecules by tumor cells and activation of those sensitizers by thermal neutrons as an external radiation source. The neutron capture reaction with the boron-10 nucleus yields high linear energy transfer (LET) particles, ⁴H and ⁷Li, with a range of 5–9 μm, thus BNCT has been expected as a cell-selective radiation therapy with the potential to control local recurrences of malignant tumors. For successful therapy, boron concentrations in the tumor of around 20–30 ppm are required with sufficiently low toxicity.^{7–13} Therefore, development of efficient boron delivery to tumors is still an important requirement in BNCT. Various nano carrier-based BDS approaches have been employed for

the targeting of boron to tumors.¹⁴ In particular, liposomes are a promising approach as they can carry relatively large quantities of boron compounds with selective localization in tumors.^{15–18}

We have focused on the structures of phosphorous lipids in the liposomal bilayer and first developed the boron cluster lipid.¹⁹ Although the liposomes prepared from the *nido*-carborane lipid accumulated in the tumor,²⁰ their acute toxicity became a serious problem at 14 mg boron per kg body weight in mice.^{20,21} We succeeded in the replacement of the *nido*-carborane by *closo*-dodecaborate in the boron cluster lipids.^{22,23} The liposomes prepared the *closo*-dodecaborate lipids did not display acute toxicity for up to 30 mg boron per kg body weight in mice²⁴ and a boron concentration of 23 ppm in the tumor with a tumor/blood ratio of ~2 was observed 24 h after administration of the distearoylphosphatidyl boron lipid (DSBL)-25% PEG liposomes.²⁵ Symmetric *closo*-dodecaborate lipids and monoanionic *closo*-dodecaborate lipids have been recently developed as candidates for liposomal boron delivery vehicles.^{26–28} Therefore, a boron delivery system (BDS) to tumors using boron-lipid liposomes has become one of the most promising approaches for BNCT. In BDS, it is very important to know detailed boron biodistribution in tissues because the distributions of tumor cells are often heterogeneous and liposomes may spread over a certain distance from tumoral blood vessels. Although the boron concentration in each tissue has been determined using inductively coupled plasma (ICP) or γ -prompradiography, a cell-level distribution of boron lipid liposomes has not been studied yet. In this paper, we report the design and synthesis of fluorescence-labeled *closo*-dodecaborane lipids (FL-SBL) (see Fig. 1) and the preparation of FL-SBL-labeled DSPC liposomes. We preliminarily demonstrated an *in vivo* biodistribution experiment of the FL-SBL-labeled DSPC liposomes using tumor-bearing mice.

Department of Chemistry, Faculty of Science, Gakushuin University, 1-5-1 Mejiro, Toshima-ku, Tokyo, 171-8588, Japan. E-mail: hiroyuki.nakamura@gakushuin.ac.jp; Fax: (+81) (0)3 5992 1029; Tel: (+81) (0)3 3986 0221
† Electronic supplementary information (ESI) available: spectral data for new compounds. See DOI: 10.1039/c1ob06500a

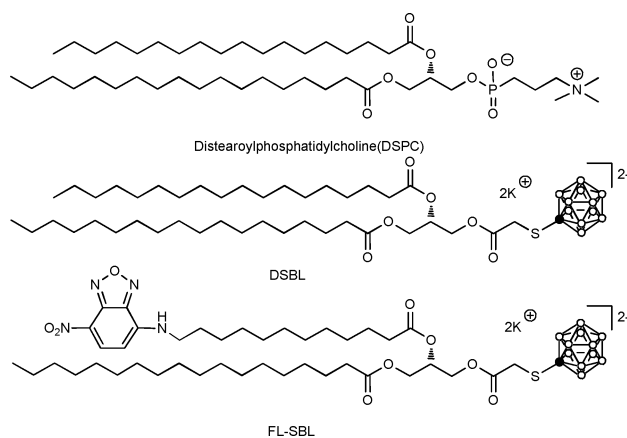
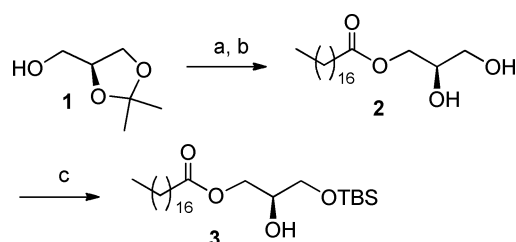


Fig. 1 Structures of distearoylphosphatidylcholine (DSPC), *closo*-dodecaborate lipid (DSBL), and fluorescence-labeled *closo*-dodecaborate lipid (FL-SBL).

Results and discussion

Synthesis

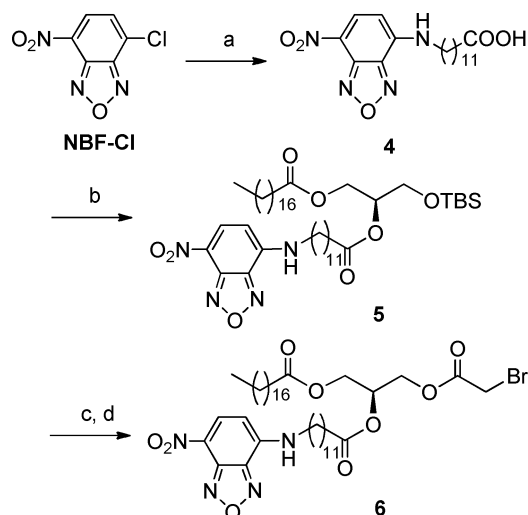
Synthesis of the hydrophobic tail function of FL-SBL is shown in Scheme 1. The coupling reaction of (S)-(+)-1,2-isopropylidenglycerol (**1**) with stearic acid proceeded in the presence of dicyclohexylcarbodiimide (DCC) and *N,N*-dimethylaminopyridine (DMAP) in CHCl_3 to give the corresponding ester, which was treated with Amberlyst 15 in $\text{MeOH}/\text{CH}_2\text{Cl}_2$ (1 : 1) to afford the diol **2** in 88% yield in two steps.²⁹ Selective protection of the primary alcohol in the diol **2** with TBSCl gave the corresponding silyl ether **3** in 85% yield.



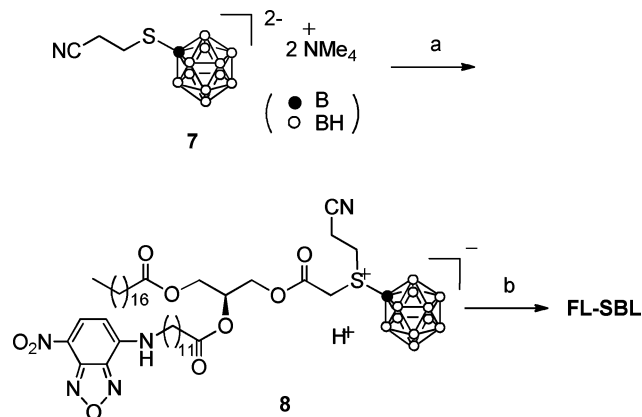
Scheme 1 Reagents and conditions: (a) octadecanoic acid, DMAP, DCC, CHCl_3 , 88%; (b) Amberlyst 15, $\text{MeOH}/\text{CH}_2\text{Cl}_2$, quant; (c) TBDMSCl, imidazole, THF, 85%.

We next synthesized the fluorescent tail of the boron lipid. We chose 4-amino-7-nitrobenzofurazan (NBF) as a fluorescent moiety and introduced it into one of two tails in DSBL, as shown in Scheme 2. The reaction of chloro-7-nitrobenzofurazan with 12-aminododecanoic acid proceeded in the presence of NaHCO_3 in ethanol to afford the corresponding NBF-conjugated decanoic acid **4** in 56% yield.³⁰ The coupling reaction of **3**^{29,31} with **4** gave the fluorescence-labeled hydrophobic tail function **5** in 55% yield. Removal of the TBS group in compound **5**, followed by ester formation with bromoacetyl bromide afforded the fluorescence-labeled lipid precursor **6** in 68% yield in two steps.

Scheme 3 shows the conjugation of a *closo*-dodecaborate moiety to the precursor **7** using the protected BSH **8**, which was prepared from BSH according to Gabel's protocol. Briefly, BSH was reacted with 2-bromopropionitrile (2 equiv.) in $\text{CH}_3\text{CN}/\text{H}_2\text{O}$



Scheme 2 Reagents and conditions: (a) 12-aminododecanoic acid, NaHCO_3 , EtOH, 37 °C, 56%; (b) **3**, DCC, DMAP, CHCl_3 , 55%; (c) HF-pyridine, pyridine, THF; (d) bromoacetyl bromide, pyridine, CHCl_3 , 68% in two steps.



Scheme 3 Reagents and conditions: (a) i. **7**, CH_3CN , ii. chromatography on SiO_2 , 23%; (b) *t*-BuOK, THF, 49%.

(1 : 1) and the resulting S-dialkylated dodecaborate was treated with tetramethylammonium hydroxide in dry THF to give the protected BSH **8**. S-Alkylation of **8** with the precursor **7** proceeded in acetonitrile under reflux gave the corresponding S-dialkylated product **9**, which was treated with potassium *tert*-butoxide in dry THF to afford the fluorescence-labeled *closo*-dodecaborane lipid FL-SBL.

Characterization of FL-SBL liposomes

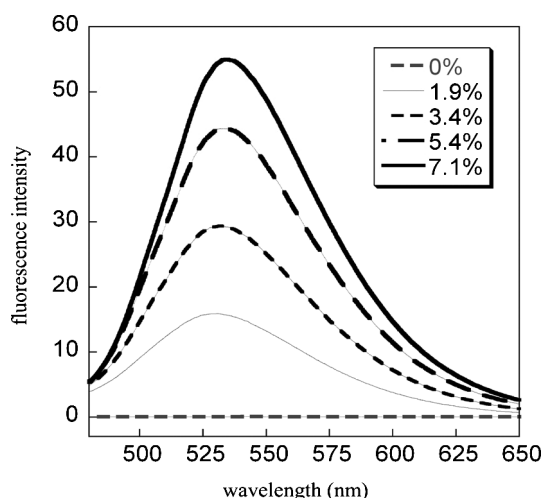
PEG units conjugated on the surface of liposomes are important for a prolonged residence time in the circulation and escaping ability from RES uptake, promoting the extravasation of the liposomes into the solid tumor tissue for the liposomal drug delivery system. Therefore, we prepared PEG-conjugated FL-SBL-labeled DSPC liposomes by means of post-insertion of various amounts of FL-SBL into PEGylated DSPC liposomes. The boron and phosphorus concentration in the liposome solutions and their diameter and zeta potential were measured. The results are summarized in Table 1. The PEGylated DSPC

Table 1 Boron and phosphorus concentrations, particle size, and zeta potential of the FL-SBL-labeled PEGylated DSPC liposomes

Volume of FL-SBL (μL)	Boron conc. (ppm)	Phosphorus conc. (ppm)	B/P ratio (%)	Particle size (nm)	Zeta potential (mV)
0	—	1876.2	0	97.2 ± 0.15	4.10 ± 0.35
10	41.3	2153.4	1.9	97.6 ± 0.47	23.2 ± 2.35
20	73.8	2169.2	3.4	97.4 ± 0.20	23.3 ± 3.04
30	112.6	2066.1	5.4	96.2 ± 1.38	21.1 ± 1.70
40	146.7	2054.5	7.1	97.8 ± 1.15	20.0 ± 3.52

liposomes prepared from DSPC, CH, and DSPE-PEG-OME (1 : 1 : 0.11, molar ratio) by REV method displayed 97.22 nm in diameter with -29.3 mV of zeta potential. Then various volumes (10–40 μL) of the FL-SBL solution (10 mg mL^{-1}) were mixed with 500 μL of the primary prepared PEGylated DSPC liposome solution (1876 ppm P concentration). Free FL-SBL was removed from the resulting liposome solutions by ultracentrifugation at 200,000 g for 60 min. With the increase in volume of the additive FL-SBL solution, the boron concentration in the liposomes increased. The boron/phosphorus concentration ratio increased roughly in proportion from 1.9 to 7.1% w/w without affecting their particle size. However, addition of the FL-SBL solution increased the zeta potential of each liposome from -29.3 to -20.0 mV. Our previous results showed that the zeta potential of the 5% DSBL liposomes is -42.8 mV and an increase in the anionic DSBL lipid contents resulted in more anionic liposome formation.²⁵ Since the current liposomes contain the PEG function, the aqueous surface layers of liposomes formed by the PEG function would involve the counter cations of negatively charged FL-SBL. Thus, the PEGylated DSPC liposomes became more cationic by addition of FL-SBL.

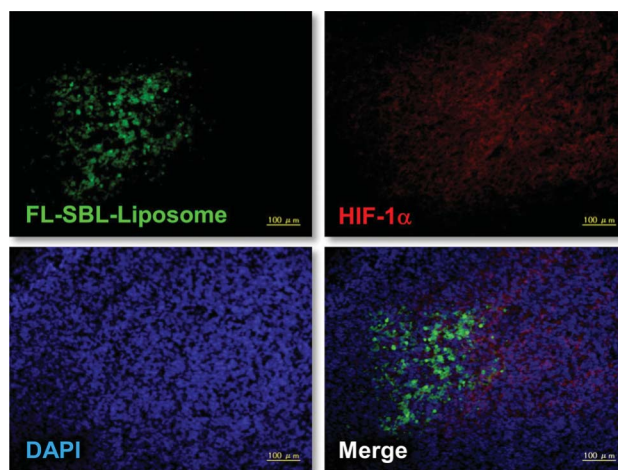
We next investigated a concentration-dependent increase in fluorescence intensity of the FL-SBL-labeled DSPC liposomes. The fluorescence intensity was measured at a range of emission wavelengths from 475 to 650 nm using an excitation wavelength of 460 nm. As shown in Fig. 2, the maximum emission wavelength of FL-SBL-labeled DSPC liposomes appeared at 531 nm and the fluorescent intensities increased along with increase of the boron/phosphorus concentration ratios that are indicated in Table 1. A slight shift in the wavelength of maximum fluorescence

**Fig. 2** Dose-dependent increase of fluorescence intensity of the FL-SBL-labeled PEGylated liposomes.

emission toward higher wavelength was observed along with increase of a concentration of FL-SBL in the liposome membrane.

In vivo imaging

We next examined the *in vivo* biodistribution of the FL-SBL-labeled liposomes using the colon 26 tumor-bearing mice. The tumor-bearing mice were injected *via* the tail vein with 200 μL of FL-SBL-labeled liposomes. After 36 h, the tumor was excised and frozen in O.C.T. embedding compound, and a cryostat section was prepared for immunofluorescent staining. Fig. 3 shows the fluorescence microscopy images of cryostat sections of tumor tissues injected with the FL-SBL-labeled liposomes (green) and cell nuclei were stained with DAPI (blue). Hypoxic cells were visualized by immunofluorescent staining with an endogenous marker of tumor hypoxia, anti-HIF-1 α antibody (red). Interestingly, the distribution of the FL-SBL-labeled liposomes did not overlap with the localization of hypoxic cells. In general, hypoxic cells are located a certain distance from blood vessels (>150 μm) because of the low oxygen supply. Therefore, the current results may indicate that the liposomes are delivered to the tumor tissue but not distributed to hypoxic tissue which is located far from the blood supply in the tumor. Previously we reported the BNCT effect of tumor-bearing mice injected with dodecaborate lipid (DSBL) liposomes.²⁵ Tumor growth inhibition was observed a week after neutron irradiation, however, re-growth of the tumor

**Fig. 3** *In vivo* imaging of the FL-SBL-labeled liposomes in the colon 26 tumor-bearing mice. The tumor-bearing mice were injected *via* the tail vein with 200 μL of FL-SBL-labeled liposomes. After 36 h, the tumor tissues were stained with DAPI (blue). Immunofluorescent staining (red) was carried out with an endogenous marker of tumor hypoxia, anti-HIF-1 α antibody. Distribution of the FL-SBL-labeled liposomes in tumor tissue was visualized by green.

was also observed after two weeks. It is known that HIF-1 α is a key regulator of the expression of various genes associated with tumor angiogenesis, metastasis, invasion, proliferation and apoptosis.³² HIF-1 α is implicated in treatment resistance and poor prognosis in the hypoxic region around the cancer. Therefore, delivery of drugs into tissues located far from blood vessels has been considered as an important issue for successful drug targeting in drug delivery systems.³³ In this regard, delivery of boron to the hypoxic region is also an important issue for the achievement of efficient BNCT of cancers.

Conclusion

We succeeded in the synthesis of the fluorescence-labeled *closo*-dodecaborane lipid, FL-SBL, which was readily accumulated into the PEGylated DSPC liposomes prepared from DSPC, CH, and DSPE-PEG-OMe by the post insertion protocol. The boron concentrations and the fluorescence intensities of the resulting FL-SBL-labeled DSPC liposomes increased with an increase of the additive FL-SBL and the maximum emission wavelength of the liposomes appeared at 531 nm. A preliminary *in vivo* imaging study of the boron liposomes using colon 26 tumor-bearing mice showed that the boron liposomes are delivered to the tumor tissue but not distributed to hypoxic tissue which is located far from the blood supply in the tumor. In our previous study, we found that boron concentrations in various organs became undetectably low within three weeks after injection.²⁵ Thus, we can demonstrate the stability of the boron lipids under biological conditions after accumulation in organs using FL-SBL. If the dodecaborate moiety and fatty acid moieties of FL-SBL are readily cleaved under biological conditions, the fluorescent-conjugated fatty acids are accumulated in tissues and detectable by fluorescent microscopic analysis although boron concentration is low. Although more detailed biodistribution studies are necessary to clarify the behavior of boron liposomes *in vivo*, the current investigation involves an important aspect for further development of liposomal boron delivery systems in BNCT.

Experimental section

¹H NMR and ¹³C NMR spectra were measured on JEOL JNM-AL 300 (300 MHz) and VARIAN UNITY-INOVA 400 (400 MHz) spectrometers. Chemical shifts in the ¹H and ¹³C NMR spectra were expressed in parts per million (ppm, δ units) and coupling constant was expressed in units of hertz (Hz). IR spectra were measured on a Shimadzu FTIR-8200A spectrometer. High-resolution mass spectra (ESI) were recorded on a Bruker Daltonics micro TOF-15 focus. Elemental analyses were performed by a CE instrument EA1110 CHNS-O automatic elemental analyzer. Analytical thin-layer chromatography (TLC) was performed on a glass plates (Merck Kieselgel 60 F₂₅₄, layer thickness 0.2 mm). Column chromatography was performed on silica gel (Merck Kieselgel 70–230 mesh). All reactions were carried out under argon atmosphere using standard Schlenk techniques. Most chemicals and solvents were of analytical grade and used without further purification. Distearoylphosphatidylcholine (DSPC) (COATSOME MC-8080) and DSPE-PEG-OMe (DSPE-020C) were supplied by Nippon Oil and Fats (Tokyo, Japan).

(R)-(2,2-Dimethyl-1,3-dioxolan-4-yl)methyl stearate

To a solution of (S)-(+)-1,2-isopropylidene-glycerol (**1**) (2.00 g, 15.1 mmol) in chloroform (20 mL) were added stearic acid (4.85 g, 17.1 mmol), 4-dimethylaminopyridine (DMAP: 2.09 g, 17.1 mmol) and the mixture was stirred for 25 min. To this reaction mixture was added dicyclohexylcarbodiimide (DCC: 3.53 g, 17.1 mmol) in chloroform (12 mL) dropwise and the mixture was further stirred for 2 h at room temperature. The mixture was filtered with celite and the filtrate was concentrated under reduced pressure. The residue was purified by silica gel column chromatography with hexane/ethyl acetate (50:1) to give (R)-(2,2-dimethyl-1,3-dioxolan-4-yl)methyl stearate as a white solid (6.00 g, 1.51 mmol, 88%): ¹H NMR (400 MHz; CDCl₃) δ 4.35–4.29 (m, 1H), 4.16 (dd, J = 11.2, 4.4 Hz, 1H), 4.08 (ddd, J = 8.8, 6.0 Hz, 2H), 3.74 (dd, J = 7.4 Hz, 1H), 2.34 (t, J = 7.6 Hz, 2H), 1.64–1.61 (m, 2H), 1.44 (s, 3H), 1.37 (s, 3H), 1.28–1.25 (m, 28H), 0.88 (t, J = 6.4 Hz, 3H); ¹³C NMR (75 MHz, CDCl₃) δ 173.7, 109.8, 73.7, 66.3, 64.5, 34.1, 31.9, 29.7, 29.4, 29.3, 26.7, 25.4, 24.9, 22.7, 14.1; IR (KBr) 2920, 2851, 1736 cm⁻¹; MS (ESI) m/z 421 ([M+Na]⁺); Anal. Calcd for C₂₄H₄₆O₄: C, 72.31; H, 11.63. Found: C, 72.06; H, 11.55.

(R)-2,3-Dihydroxypropyl stearate (2)

(R)-(2,2-Dimethyl-1,3-dioxolan-4-yl)methyl stearate (7.00 mg, 17.6 mmol) was dissolved in methanol (60 mL) and dichloromethane (30 mL) and Amberlyst 15 (11.7 g) was added. The mixture was stirred under reflux for 2 h and then the resin was removed by filtration. The solvents were evaporated under reduced pressure and the residue was purified by silica gel column chromatography with hexane/ethyl acetate (5:1) to give (R)-2,3-dihydroxypropyl stearate (**2**) as a white solid (6.31 g, 17.6 mmol, quant): ¹H NMR (400 MHz; CDCl₃) δ 4.24–4.13 (m, 1H), 3.99–3.92 (m, 1H), 3.73–3.58 (m, 3H), 2.37–2.28 (m, 2H), 1.63–1.61 (m, 2H), 1.28–1.26 (m, 28H), 0.88 (t, J = 6.8 Hz, 3H); ¹³C NMR (75 MHz, CDCl₃) δ 174.3, 70.2, 65.1, 63.3, 34.1, 31.9, 29.6, 29.4, 29.1, 24.8, 22.6, 14.0; IR (KBr) 2920, 2851, 1732, 1180 cm⁻¹; MS (ESI) m/z 359 ([M+H]⁺), 381 ([M+Na]⁺); Anal. Calcd for C₂₁H₄₂O₄: C, 70.34; H, 11.81. Found: C, 70.46; H, 11.86.

3-O-Stearoyl-1-O-(tert-butyl-dimethyl-silyl)-sn-glycerol (3)

To a mixture of **2** (3.22 g, 8.98 mmol) and imidazole (0.88 g, 12.5 mmol) in THF (50 mL) was added a THF (25 mL) solution of *tert*-butyldimethylsilyl chloride (1.51 g, 9.99 mmol) dropwise and the mixture was stirred for 2 h under reflux. The solvent was removed under reduced pressure and the residue was purified by silica gel column chromatography with hexane/ethyl acetate (20:1) to give 3-*O*-stearoyl-1-*O*-(*tert*-butyl-dimethyl-silyl)-*sn*-glycerol (**3**) as a white solid (3.60 g, 7.61 mmol, 85%): ¹H NMR (400 MHz; CDCl₃) δ 0.08 (s, 6H), 0.88 (t, J = 6.8 Hz, 3H), 0.90 (s, 9H), 1.25 (s, 28H), 1.60–1.64 (m, 2H), 2.34 (t, J = 7.6 Hz, 2H), 3.67 (dd, J = 9.4 Hz, J = 18.8 Hz, 2H), 3.86–3.89 (m, 1H), 4.09–4.18 (m, 2H); ¹³C NMR (300 MHz; CDCl₃) δ -5.47, 14.10, 18.26, 22.68, 24.94, 25.82, 29.14, 29.26, 29.35, 29.45, 29.68, 31.92, 34.20, 63.70, 64.98, 70.01, 173.95; IR (CHCl₃) 2928, 2856, 1734, 1464, 1258, 1177, 1096 cm⁻¹; MS (ESI) m/z 496 ([M+Na]⁺); Anal. Calcd for C₂₇H₅₆O₄Si: C, 68.59; H, 11.94. Found: C, 68.89; H, 11.81.

12-(7-Nitrobenzo[c][1,2,5]oxadiazol-4-ylamino)dodecanoic acid (4)

To a solution of NaHCO₃ (4.21 g, 50 mmol) in water (125 mL) was added an ethanol solution (325 mL) of 12-aminododecanoic acid (2.70 g, 12.5 mmol) at 37 °C and the mixture was stirred for 10 min. Chloro-7-nitrobenzofurazan (5.02 g, 25 mmol) was added and then the reaction mixture was stirred at 37 °C for overnight with light shielding. The reaction was quenched by adding HCl (1 M, 56 mL) and the reaction mixture was extracted with chloroform. The organic layer was washed with water, dried over anhydrous sodium sulfate, and then concentrated. The residue was purified by silica gel column chromatography with hexane/ethyl acetate (20 : 1) to give **4** as an orange solid (2.65 g, 7.01 mmol, 56%): ¹H NMR (400 MHz; CDCl₃) δ 8.51 (d, *J* = 8.8 Hz, 1H), 6.18 (d, *J* = 8.4 Hz, 1H), 3.48 (dd, *J* = 9.2, 15.2 Hz, 2H), 2.36 (t, *J* = 7.6 Hz, 2H), 1.83–1.47 (m, 4H), 1.30 (s, 14H); ¹³C NMR (75 MHz, CDCl₃) δ 178.5, 144.3, 143.9, 136.5, 124.2, 124.0, 98.5, 44.0, 33.7, 29.3, 29.1, 28.9, 28.5, 26.9, 24.6; IR (KBr) 3356, 3244, 2924, 2851, 1709, 1620, 1269, 1188, 1126 cm⁻¹; MS (ESI, positive) *m/z* 379 ([M+H]⁺), 401 ([M+Na]⁺), 417 ([M+K]⁺), 377 ([M-H]⁻); HRMS (ESI, positive) *m/z* calcd. for C₁₈H₂₆N₄O₅ [M+Na]⁺: 401.1801, found: 401.1804.

(S)-3-(tert-Butyldimethylsilyloxy)-2-(12-(7-nitrobenzo[c][1,2,5]-oxadiazol-4-ylamino)dodecanoyloxy)propyl stearate (5)

To a mixture of **4** (0.19 g, 0.5 mmol) and *N*-methylimidazole (0.12 mL, 1.5 mmol) in dichloromethane (2.6 mL) was added a dichloromethane solution (1 mL) of tosylchloride (0.14 g, 0.7 mmol) at room temperature under argon atmosphere and the mixture was stirred for 30 min. A solution of **3** (0.24 g, 0.5 mmol) in dichloromethane (4 mL) was added to the reaction mixture and this mixture was stirred at room temperature for overnight. The reaction was quenched by water and the mixture was extracted with dichloromethane. The organic layer was washed with brine, dried over anhydrous Na₂SO₄, and concentrated. The residue was purified by silica gel column chromatography with hexane/ethyl acetate (8 : 1) to give **5** as a dark orange solid (0.23 g, 0.27 mmol, 55%): ¹H NMR (400 MHz; CDCl₃) δ 8.51 (d, *J* = 8.4 Hz, 1H), 6.18 (d, *J* = 8.8 Hz, 1H), 5.08–5.06 (m, 1H), 4.32 (dd, *J* = 12.0, 4.0 Hz, 1H), 4.16 (dd, *J* = 11.6, 6.0 Hz, 1H), 3.72 (d, *J* = 5.6 Hz, 2H), 3.49 (q, *J* = 12.4, 7.2 Hz, 2H), 2.31 (ddd, *J* = 7.2, 2.4 Hz, 4H), 1.81 (quint, *J* = 6.8 Hz, 1H), 1.61–1.42 (m, 5H), 1.29–1.25 (m, 42H), 0.88 (s, 12H), 0.05 (s, 6H); ¹³C NMR (100 MHz, CDCl₃) δ 173.4, 173.0, 144.2, 143.8, 136.4, 123.7, 98.4, 71.6, 62.3, 61.3, 43.9, 34.2, 34.1, 31.8, 29.6, 29.3, 29.1, 28.4, 26.8, 25.7, 24.8, 22.6, 18.1, 14.0, -5.5; IR (neat) 3329, 2924, 2855, 1744, 1620, 1350, 1312, 1258, 1157, 1119, 1038 cm⁻¹; MS (ESI, positive) *m/z* 856 ([M+Na]⁺), 872 ([M+K]⁺); HRMS (ESI, positive) *m/z* calcd. for C₄₅H₈₀N₄O₈Si [M+Na]⁺: 855.5643, found: 855.5641.

(S)-3-(2-Bromoacetoxy)-2-(12-(7-nitrobenzo[c][1,2,5]oxadiazol-4-ylamino)dodecanoyloxy)propyl stearate (6)

To a solution of **5** (1.08 g, 1.3 mmol) in THF (10 mL) was added tetrabutylammonium fluoride (TBAF, 1 M in 1% water containing THF, 1.4 mL) at room temperature and the mixture was stirred for 7 h. The mixture was concentrated under the reduced pressure and dissolved in ethyl acetate. The mixture was washed with water, dried over anhydrous MgSO₄, and then concentrated. The residue was passed through a short silica gel column chromatography

eluted with hexane/ethyl acetate (1 : 2) to give the crude product, which was dissolved in chloroform (10 mL). Pyridine (0.12 mL, 1.52 mmol) and bromoacetyl bromide (0.13 mL, 1.52 mmol) were added at 0 °C and the mixture was stirred for 4 h at room temperature. The precipitates were filtered using celite pad and the filtrate was concentrated *in vacuo*. The residue was purified by silica gel column chromatography with hexane/ethyl acetate (5 : 1) to give **6** as a dark orange solid (0.74 g, 0.88 mmol, 68%): ¹H NMR (400 MHz; CDCl₃) δ 8.51 (d, *J* = 8.4 Hz, 1H), 6.18 (d, *J* = 8.4 Hz, 1H), 5.30 (sext, *J* = 4.8 Hz, 1H), 4.45–4.24 (m, 2H), 4.20–4.16 (m, 2H), 3.85 (s, 2H), 3.49 (q, *J* = 12.8, 6.4 Hz, 2H), 2.34–2.31 (m, 4H), 1.81 (quint, *J* = 7.2 Hz, 2H), 1.61–1.45 (m, 4H), 1.29–1.25 (m, 42H), 0.88 (t, *J* = 6.4 Hz, 3H); ¹³C NMR (100 MHz, CDCl₃) δ 172.9, 166.5, 166.2, 143.9, 143.6, 136.5, 122.5, 98.2, 68.2, 63.5, 61.4, 43.8, 33.6, 33.0, 31.5, 30.5, 29.3, 29.0, 28.0, 26.6, 25.0, 24.5, 22.3, 13.7; IR (neat) 3333, 3078, 2920, 2855, 1747, 1620, 1350, 1273, 1165, 1119, 1045 cm⁻¹; MS (ESI, positive) *m/z* 863 ([M+Na]⁺), 879 ([M+K]⁺); HRMS (ESI, positive) *m/z* calcd. for C₄₁H₆₇BrN₄O₉ [M+Na]⁺: 861.3989, found: 861.3989.

Compound 8

A mixture of **6** (0.94 g, 1.1 mmol) and **7** (0.41 g, 1.1 mmol)³⁴ was dissolved in anhydrous acetonitrile (12 mL) at room temperature under argon atmosphere and the mixture was stirred under reflux for overnight. The solvent was removed under the reduced pressure and the residue was purified by silica gel column chromatography with hexane/ethyl acetate (1 : 2) to give **8** as dark orange oil (0.25 g, 0.25 mmol, 23%): ¹H NMR (400 MHz; CDCl₃) δ 8.45 (d, *J* = 8.0 Hz, 1H), 6.28 (d, *J* = 8.8 Hz, 1H), 5.26–5.25 (m, 1H), 4.37–3.87 (m, 4H), 3.48 (s, 2H), 3.37–3.27 (m, 4H), 3.00–2.97 (m, 2H), 2.32–2.26 (m, 4H), 1.72 (quint, *J* = 7.2 Hz, 4H), 1.56–1.54 (m, 2H), 1.28–1.24 (m, 42H), 0.86 (t, *J* = 8.0 Hz, 3H); ¹³C NMR (100 MHz, CD₃OD) δ 174.8, 166.6, 159.2, 146.2, 145.4, 138.7, 122.3, 118.2, 100.0, 69.9, 63.0, 62.7, 44.9, 44.6, 38.5, 34.9, 34.7, 32.8, 30.6, 30.2, 30.0, 27.8, 25.7, 23.5, 16.2, 14.4; IR (neat) 3564, 3329, 3082, 2909, 2851, 1732, 1620, 1180, 1119, 1045, 1003 cm⁻¹; MS (ESI, negative) *m/z* 987 ([M-H]⁻); HRMS (ESI, negative) *m/z* calcd. for C₄₅H₈₃B₁₂N₅O₉S [M-H]⁻: 988.6950, found: 988.6953.

Fluorescence-labeled *closo*-dodecaborane lipid (FL-SBL)

Compound **8** (0.15 g, 0.15 mmol) was dissolved in dried THF (10 mL) and a THF (4 mL) solution of *t*-BuOK (0.026 g, 0.22 mmol) was added dropwise. The reaction progress was monitored by thin layer chromatography (TLC). The solvent was removed under reduced pressure and the residue was purified by silica gel column chromatography with hexane/ethyl acetate (1 : 2) to give **FL-SBL** as dark orange oil (0.075 g, 0.074 mmol, 49%): ¹H NMR (400 MHz; CDCl₃) δ 8.44 (d, *J* = 8.4 Hz, 1H), 6.29 (d, *J* = 8.4 Hz, 1H), 5.20–5.15 (m, 1H), 4.29–4.13 (m, 4H), 3.47–3.41 (m, 2H), 3.21 (s, 2H), 2.43–2.24 (m, 4H), 1.72–1.69 (m, 4H), 1.52 (s, 2H), 1.38–1.21 (m, 42H), 0.84 (t, *J* = 8.0 Hz, 3H); ¹³C NMR (100 MHz, CD₃CN) δ 174.1, 160.8, 145.5, 145.3, 138.3, 123.7, 122.0, 99.8, 69.8, 63.6, 62.6, 44.6, 36.0, 35.8, 34.7, 34.5, 32.5, 30.3, 29.9, 29.6, 27.5, 25.5, 23.3, 14.3; IR (neat) 3568, 3422, 3321, 3082, 2924, 2855, 1732, 1620, 1269, 1188, 1161, 1123, 1053 cm⁻¹; MS (ESI, negative) *m/z* 466 ([M-2K]/2)²⁻; HRMS (ESI, negative) *m/z* calcd. for C₄₁H₇₈B₁₂K₂N₄O₉S [(M-2K)/2]²⁻: 467.3303, found: 467.3305.

Preparation and characterization of the FL-SBL-labeled PEGylated DSPC liposomes

PEGylated DSPC-liposomes were prepared from DSPC, CH, and DSPE-PEG-OMe (1:1:0.11, molar ratio) by the reverse-phase evaporation (REV) method 30. Briefly, a mixture of DSPC (158 mg), CH (77 mg), and DSPE-PEG-OMe (64 mg) were dissolved in 10 ml of chloroform/diisopropylether mixture (1:1, v/v) in a round-bottom flask. To the lipid solution was added 5 mL of water, forming an emulsion. The volume ratio of the aqueous phase to the organic phase was maintained at 1:2. The emulsion was sonicated for 1 min (SMT Company, UH-50 Tip-type 50 W, Japan), and then the organic solvent was removed under vacuum in a rotary evaporator at 37 °C with repeated breaking down of the generated aggregate to obtain a suspension of liposomes. The liposomes obtained were subjected to extrusion 10 times through a polycarbonate membrane of 100 nm pore size (Whatman, 110605, FILTER, 0.1UM, 25 MM, Gentauro Molecular Products, Belgium), using an extruder device (Lipex Biomembrane, Canada) thermostatted at 60 °C. Purification was accomplished by ultracentrifuging at 200,000 g for 20 min at 4 °C (himac cp 80 wx, Hitachi Koki, Japan) to obtain PEGylated DSPC liposomes as a pellet. FL-SBL was dissolved in normal saline solution and various volumes (10–40 µL) of the FL-SBL solution (10 mg mL⁻¹) were mixed with 500 µL of DSPC liposome solution described above (ca. 2000 ppm P concentration). The mixture was maintained at 25 °C for 5 min and free FL-SBL was removed by ultracentrifugation at 200,000 g for 60 min at 4 °C. The obtained FL-SBL-labeled liposomes were resuspended in PBS or water. Liposome size and zeta potential were measured with an electrophoretic light scattering spectrophotometer (Nano-ZS, Sysmex, Japan). The compositions of FL-SBL and DSPC in liposomes were calculated from data obtained by the simultaneous measurement of boron and phosphorus concentrations by inductively coupled plasma atomic emission spectroscopy (ICP-AES, HORIBA, Japan). The fluorescence intensity of each sample was measured at a range of emission wavelengths from 475 to 650 nm using an excitation wavelength of 460 nm.

In vivo fluorescence imaging

Tumor-bearing mice (female, 5–6 weeks old, 16–20 g, Sankyo Labo Service, Japan) were prepared by injecting subcutaneously (s.c.) a suspension (2.5 × 10⁶ cells mouse⁻¹) of colon 26 cells directly into the back. The mice were kept on a regular chow diet and water and maintained under a 12 h light/dark cycle in an ambient atmosphere. Fluorescence imaging experiments were performed when the tumor diameter was 7 to 9 mm. The tumor-bearing mice were injected *via* the tail vein with 200 µL of FL-SBL-labeled liposomes. FL-SBL-labeled liposomes prepared from 40 µL of the FL-SBL solution (10 mg mL⁻¹) as indicated above were used for this experiment. After 36 h, the mice were anaesthetized with isoflurane and blood was removed from the retro-orbital sinus. The mice were then sacrificed by cervical dislocation and dissected, and the tumor was excised. The tumor tissue samples were frozen in O.C.T. embedding compound, and a cryostat section was prepared for immunofluorescent staining. Antibodies used were anti-HIF-1α antibody (BD Transduction Laboratories, Lexington, KY) and

Rhodamine-conjugated secondary antibody (Santa Cruz). The samples were coverslipped using Vectashield mounting medium (Vector Laboratories, USA) for further analysis under a fluorescence confocal microscope (FV100D IX81, OLYMPUS, Japan). All experiments using mice were performed in compliance with the relevant laws and institutional guidelines approved by the Institutional Animal Care and Use Committee in Gakushuin University.

Acknowledgements

We thank Professor Yoshiyuki Inaguma (Gakushuin University) for the measurement of concentration-dependent increase of fluorescent intensity of the FL-SBL-labeled PEGylated DSPC liposomes. This work was supported in part by Health and Labour Sciences Research Grants for Research on Nanotechnical Medical from the Ministry of Health, Labour and Welfare (20100201) and the Ministry of Education, Science, Sports, Culture and Technology, Grant-in-Aid for Scientific Research (B) (No. 23390018) from Japan.

Notes and references

- 1 Y. Matsumura and H. Maeda, *Cancer Res.*, 1986, **46**, 6387–6392.
- 2 H. Maeda, J. Wu, T. Sawa, Y. Matsumura and K. Hori, *J. Controlled Release*, 2000, **65**, 271–284.
- 3 D. F. Emerich and C. G. Thanos, *Biomol. Eng.*, 2006, **23**, 171–184.
- 4 O. M. Koo, I. Rubinstein and H. Onyuksel, *Nanomed.: Nanotechnol., Biol. Med.*, 2005, **1**, 193–212.
- 5 A. K. Iyer, G. Khaled, J. Fang and H. Maeda, *Drug Discovery Today*, 2006, **11**, 812–818.
- 6 K. Greish, *J. Drug Targeting*, 2007, **15**, 457–464.
- 7 R. F. Barth, A. H. Soloway, R. G. Fairchild and R. M. Brugger, *Cancer*, 1992, **70**, 2995–3007.
- 8 Y. Mishima, M. Ichihashi, S. Hatta, C. Honda, K. Yamamura and T. Nakagawa, *Pigm. Cell Res.*, 1989, **2**, 226–234.
- 9 Y. Nakagawa and H. Hatanaka, *J. Neuro-Oncol.*, 1997, **33**, 105–115.
- 10 I. Kato, K. Ono, Y. Sakurai, M. Ohmae, A. Maruhashi, Y. Imahori, M. Kirihata, M. Nakazawa and Y. Yura, *Appl. Radiat. Isot.*, 2004, **61**, 1069–1073.
- 11 R. F. Barth, *Appl. Radiat. Isot.*, 2009, **67**, S3–S6.
- 12 R. F. Barth, A. H. Soloway and R. M. Brugger, *Cancer Invest.*, 1996, **14**, 534–550.
- 13 A. H. Soloway, W. Tjarks, B. A. Barnum, F. G. Rong, R. F. Barth, I. M. Codogni and J. G. Wilson, *Chem. Rev.*, 1998, **98**, 1515–1562.
- 14 Z. Yinghuai, K. Cheng Yan, J. A. Maguire and N. S. Hosmane, *Curr. Chem. Biol.*, 2007, **1**, 141–149.
- 15 D. A. Feakes, K. Shelly, C. B. Knobler and M. F. Hawthorne, *Proc. Natl. Acad. Sci. U. S. A.*, 1994, **91**, 3029–3033.
- 16 H. Yanagie, T. Tomita, H. Kobayashi, Y. Fujii, Y. Nonaka, Y. Saegusa, K. Hasumi, M. Eriguchi, T. Kobayashi and K. Ono, *Br. J. Cancer*, 1997, **75**, 660–665.
- 17 K. Maruyama, O. Ishida, S. Kasaoka, T. Takizawa, N. Utoguchi, A. Shinohara, M. Chiba, H. Kobayashi, M. Eriguchi and H. Yanagie, *J. Controlled Release*, 2004, **98**, 195–207.
- 18 D. A. Feakes, K. Shelly and M. F. Hawthorne, *Proc. Natl. Acad. Sci. U. S. A.*, 1995, **92**, 1367–1370.
- 19 H. Nakamura, Y. Miyajima, T. Takei, S. Kasaoka and K. Maruyama, *Chem. Commun.*, 2004, 1910–1911.
- 20 Y. Miyajima, H. Nakamura, Y. Kuwata, J.-D. Lee, S. Masunaga, K. Ono and K. Maruyama, *Bioconjugate Chem.*, 2006, **17**, 1314–1320.
- 21 T. Li, J. Hamdi and M. F. Hawthorne, *Bioconjugate Chem.*, 2006, **17**, 15–20.
- 22 J.-D. Lee, M. Ueno, Y. Miyajima and H. Nakamura, *Org. Lett.*, 2007, **9**, 323–326.
- 23 H. Nakamura, M. Ueno, H. S. Ban, K. Nakai, K. Tsuruta, Y. Kaneda and A. Matsumura, *Appl. Radiat. Isot.*, 2009, **67**, S84–S87.
- 24 H. Nakamura and D. Nejat, in *Methods Enzymol.*, Academic Press, 2009, vol. Volume 465, pp. 179–208.

- 25 M. Ueno, H. S. Ban, K. Nakai, R. Inomata, Y. Kaneda, A. Matsumura and H. Nakamura, *Bioorg. Med. Chem.*, 2010, **18**, 3059–3065.
- 26 E. Justus, D. Awad, M. Hohnholt, T. Schaffran, K. Edwards, G. Karlsson, L. Damian and D. Gabel, *Bioconjugate Chem.*, 2007, **18**, 1287–1293.
- 27 T. Schaffran, A. Burghardt, S. Barnert, R. Peschka-Su's, R. Schubert, M. Winterhalter and D. Gabel, *Bioconjugate Chem.*, 2009, **20**, 2190–2198.
- 28 T. Schaffran, F. Lissel, B. Samatanga, G. A. Karlsson, A. Burghardt, K. Edwards, M. Winterhalter, R. Peschka-Süss, R. Schubert and D. Gabel, *J. Organomet. Chem.*, 2009, **694**, 1708–1712.
- 29 R. J. Kubiak and K. S. Bruzik, *J. Org. Chem.*, 2003, **68**, 960–968.
- 30 J. C. McIntyre, D. Watson and R. G. Sleight, *Chem. Phys. Lipids*, 1993, **66**, 171–180.
- 31 C. E. Burgos, D. E. Ayer and R. A. Johnson, *J. Org. Chem.*, 1987, **52**, 4973–4977.
- 32 G. L. Semenza, *Nat. Rev. Cancer*, 2003, **3**, 721–732.
- 33 P. Ruenraroengsak, J. M. Cook and A. T. Florence, *J. Controlled Release*, 2010, **141**, 265–276.
- 34 D. Gabel, D. Moller, S. Harfst, J. Roesler and H. Ketz, *Inorg. Chem.*, 1993, **32**, 2276–2278.